

FULL MESH WARPING TECHNIQUES

Steve Stoffels

Physics Department
University of Technology Eindhoven
stoffels@ccrma.stanford.edu

ABSTRACT

This paper discusses methods for the elimination of dispersion in a digital waveguide mesh. As in previous methods, a highly isotropic waveguide mesh is chosen as a starting point, reducing the problem to compensation of frequency-dependent dispersion. For this purpose, as an alternative to Savioja and Välimäki's technique of frequency-warping the input/output signals, we propose (1) inhomogeneous allpass-warping of delay elements, which enables use of allpass filters without introducing delay-free loops, and (2) "mass loading" the mesh in such a way that high-frequency propagation speed is increased to partially compensate dispersion due to quantization over a grid.

1. INTRODUCTION

The digital waveguide mesh [?] has been used to numerically solve the wave equation in membranes and acoustic volumes. As is well known, the waveguide mesh gives excellent performance with respect to dissipation, especially in the lossless case, but it has a *dispersion error* which varies with propagation direction and frequency [?]. This means waves at different frequencies and/or directions travel at different speeds.

The need for a waveguide mesh without dispersion error arises, e.g., in room acoustics simulations in which a 3D waveguide mesh is used to simulate the behavior of traveling waves inside the room [?]. Dispersion error is undesirable in this application since the solution for the wave equation in air exhibits a uniform speed in all directions and for all frequencies.

Choosing the *triangular* mesh in 2D helps to make the dispersion error much more uniform with respect to direction [?, ?], as does the *deinterpolated mesh* [?, ?]. Most recently, a novel *frequency warping* method has been proposed for greatly reducing dispersion error as a function of frequency [?, ?]. This paper focuses on alternative techniques for reducing dispersion error as a function of frequency.

We first consider how the delay elements in a waveguide mesh can be warped and the problems that can thus be introduced, such as delay-free loops. A novel structure is proposed which we call the *asymmetric warped waveguide mesh*. This structure consists of two different alternating single-junction cells, one which delays waves in the usual way, and the other which warps the wave speed so that it becomes more uniform.

A second method consists of adding a *load* to the junctions. The natural dispersion in a waveguide mesh slows down high-frequency propagation. "Mass loading" the mesh by means of a mass connected to each node makes it "stiffer", and this speeds up high frequencies in a partially compensating way. More generally,

a higher order load impedance can be optimized to compensate dispersion more completely.

By choosing to implement the first-order mass load in "wave digital" form, the mass becomes a simple unit-delay "self-loop" attached to each node via a single port. The "wave digital mass" can be further adjusted by placing a first-order allpass in series with the unit delay in the self-loop; this allows further tuning of dispersion reduction over a restricted frequency range.

2. OVERVIEW OF RESULTS

The warping technique introduced in [3,4] requires frequency warping the input signal to the mesh, processing the warped signal in a normal mesh, then finally unwarping the extracted output signal. Since the frequency warping is carried out using an IIR filtering process, it is limited to offline operation. It is therefore of interest to find dispersion compensation methods which can be used in real time. In general, we are looking for ways to warp the *mesh* as opposed to its input/output signals. Warping the mesh structure means that signals fed into it propagate at more or less the correct speed without having to preprocess or postprocess the input/output signals. A side benefit of compensating the mesh and not the signals is that waves may be more easily and accurately "visualized" on the mesh during simulation.

First, we will review existing methods for frequency warping to compensate for dispersion, followed by a discussion of the newly proposed techniques. We will only treat the case of the two dimensional waveguide mesh, but the basic ideas readily generalize to three or more dimensions.

3. NEARLY ISOTROPIC WAVEGUIDE MESHES

The first step is to choose a waveguide mesh having negligible dispersion error as a function of propagation direction. That is, we need an *isotropic* waveguide mesh. We are aware of two basic contenders for this purpose: the triangular waveguide mesh [?], and the deinterpolated waveguide mesh [?]. After this, the problem is reduced to finding a means of frequency-warping the isotropic waveguide mesh to compensate for dispersion as a function of frequency.

3.1. Deinterpolated Waveguide Mesh

The deinterpolated mesh is a modification of the square waveguide mesh which makes wave propagation more uniform in all directions. Starting from a square mesh we have the finite difference scheme

$$\begin{aligned}
 v_{Jl,m}(n) &+ v_{Jl,m}(n-2) \\
 &= \frac{1}{2} [v_{Jl,m+1}(n-1) + v_{Jl,m-1}(n-1) \\
 &\quad + v_{J(l+1),m}(n-1) + v_{J(l-1),m}(n-1)]
 \end{aligned}$$

This structure can be made more uniform by adding diagonal delay elements. Because these delay elements don't end at actual mesh nodes, an interpolation scheme has to be used. The finite difference scheme for this structure is given by

$$\begin{aligned}
 v_J(n) &= \frac{2}{N} \sum_{i=1}^3 \sum_{j=1}^3 h_{ij} v_{J,i,j}(n-1) - v_J(n-2) \\
 &= \frac{1}{4} \sum_{i=1}^3 \sum_{j=1}^3 h_{ij} v_{J,i,j}(n-1) - v_J(n-2)
 \end{aligned}$$

We now sum over all the eight neighbors plus the node itself. The weighting factors inside the sum are different between horizontal directions, diagonal directions and the self loop. The values of the weighting factors depend on the interpolation scheme used. Optimal results are obtained when the weighting factors are optimized with a minimization criterion for uniform dispersion.

First, the finite difference notation of the deinterpolated mesh is transformed to a waveguide mesh. This will enable us later on to use warping directly inside the mesh structure.

For the deinterpolated mesh, the junction velocities can be expressed in terms of the incoming wave variables as

$$v_J(n) = \frac{2}{8} \sum_{x=1}^3 \sum_{y=1}^3 h_{x,y} v_{x,y}^+(n)$$

where $h_{x,y}$ are the "deinterpolation coefficients". The 9-port junctions are connected by delay lines, and one of the delay lines is simply a self-loop back to the original junction. This equation makes the waveguide simulation largely isotropic. Note that the physical structure equivalent to a junction in the deinterpolated mesh is a 9-port junction with different impedances at each port and with one port being equivalent to a wave digital mass.

Von Neumann Analysis [?] on the optimal deinterpolated mesh gives the dispersion error shown in Fig. ??.

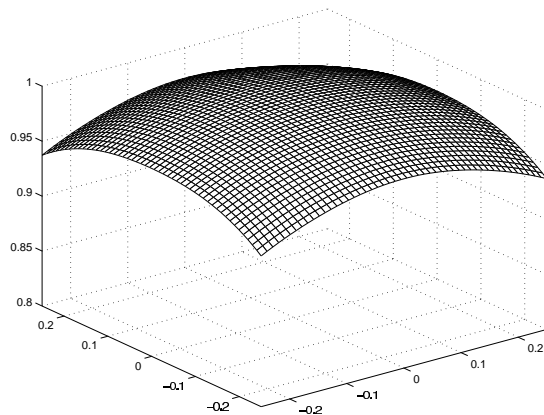
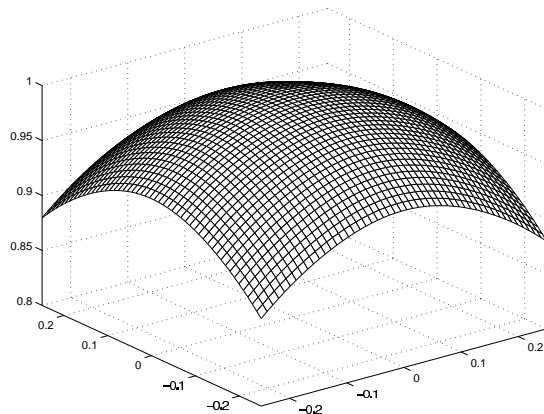
On the two horizontal axes, the spatial frequency is plotted. The vertical axis gives the dispersion error as a multiplicative factor for the ideal wave speed with no dispersion. The dispersion factor is 1 at dc (both spatial frequencies at 0). The dispersion error is almost uniform in all directions. This will be a good starting point for using warping techniques later on.

3.2. Triangular Mesh

For the triangular mesh, the junction velocities are given by

$$v_J(n) = \frac{1}{3} \sum_{i=1}^6 v_{x,y}^+(n)$$

The junctions are arranged in a triangular structure and again connected by unit delay lines. Unlike the interpolated mesh, there is



Frequency warping of a digital filter is typically achieved by replacing each delay with an allpass filter. The most commonly used allpass filter for this goal is the first-order allpass filter:

$$A(z) = \frac{z^{-1} + \lambda}{1 + \lambda z^{-1}} \quad (1)$$

Unwarping is accomplished by replacing λ by $-\lambda$. To frequency-warp a time signal $x(n), n = 0, 1, 2, \dots, N - 1$, a length N finite-impulse-response (FIR) filter is constructed having impulse response $h_n = x(n)$. Such a filter is depicted in Fig. ?? . Next, each delay element of the FIR filter is replaced by a first-order allpass $A(z)$, and the filter is fed an impulse $\delta(n) = [1, 0, 0, \dots]$. The output $y(n)$ is then the desired frequency-warped signal. The warped delay elements $A(z)$ can be viewed as providing a different sampling rate at each frequency. Since the filter is IIR, $y(n)$ must be post-windowed or truncated in some manner.

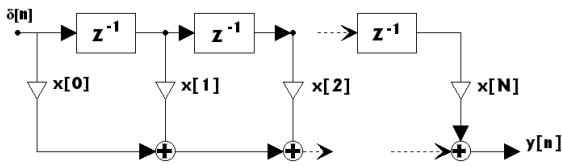


Figure 3: FIR filter structure used as a basis for signal frequency warping.

This frequency warping technique is an off-line process since the signal is preprocessed before running the simulation, and it is necessary to know the entire signal before beginning the simulation. (Since there is a delay-free path through the allpass filters $A(z)$, $y(0)$ depends on all N input samples $x(n)$.) The technique also becomes expensive when using multiple input signal and multiple pick-up points, since every signal has to be preprocessed and postprocessed. Also, exciting the mesh with an object of a given geometric shape, such as a mallet, is more difficult to work out precisely.

We therefore conclude that a need exists for a frequency warping technique that works directly on the mesh instead of on the input signal, thus eliminating the disadvantages outlined above. In the next section, some novel structures will be proposed, and their advantages and disadvantages will be discussed.

5. FREQUENCY WARPING THE WAVEGUIDE MESH

When frequency warping the mesh it can be noted that the mesh is built up using two basic components: *junctions* and *delay lines* connecting the junctions. Each can be used to warp the waveguide mesh. We will treat both separately.

5.1. Warping Delay Elements in the Mesh

The “obvious” way to warp the mesh is to replace each delay element with a first-order allpass filter

$$H_a(z) = \frac{-p + z^{-1}}{1 - pz^{-1}}$$

This seems obvious when we look at a single delay line. This first-order allpass filter can speed up waves of higher frequencies and slow down waves of lower frequencies. Thus the delay line seems shorter for higher frequency waves. In other words, we have introduced a delay line of variable length. However, since $H_a(z)$ has a delay-free path for $p \neq 0$, it introduces delay-free loops in the mesh structure. The structure is therefore not realizable in a straightforward manner.

The first-order allpass can be used in series with a sample of pure delay, thus solving the delay-free loop problem, as shown in Fig. ?? .

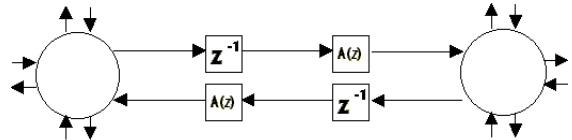


Figure 4: Delay in series with allpass filter.

However, denoting the sampling rate by $f_s = 1/T$, the extra delays $A(z)$ in the mesh reduce the useable bandwidth from $[0, f_s/4]$ (for normal waveguide meshes) down to as low as $[0, f_s/8]$ at frequencies for which the allpass filter provides close to a sample of delay .

5.2. Inhomogeneously Warped Delay Elements

Another way of warping the delay lines can be called the “asymmetrically warped waveguide mesh”. It consists of two sets of cell types which alternate, as shown in Fig. ?? . The first kind consists of a single waveguide junction with delays coming in, and first-order allpass filters going out; the second kind has allpass filters coming in and delays going out. In this kind of mesh, the signals passing through get alternately sped up and delayed. This effectively eliminates delay-free loops. It is important to note that a signal passing through is only warped every other junction, this means that the warping factor has to be twice as large as it would be in a mesh which would warp the sample at every node. This structure has the disadvantage that it is geometry dependent and can’t be easily transferred to structures other than the rectilinear waveguide mesh.

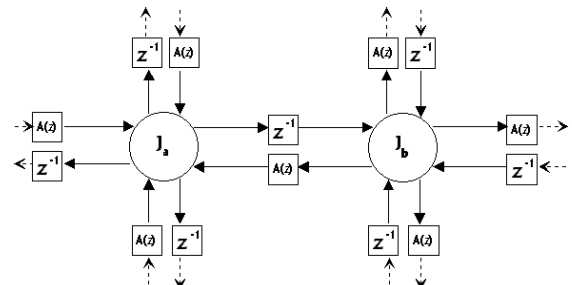


Figure 5: Asymmetrically warped waveguide mesh.

In an asymmetric structure the unit element in the mesh doesn't consist of just a single node but rather of four nodes interconnected. This is shown in Fig. ??.

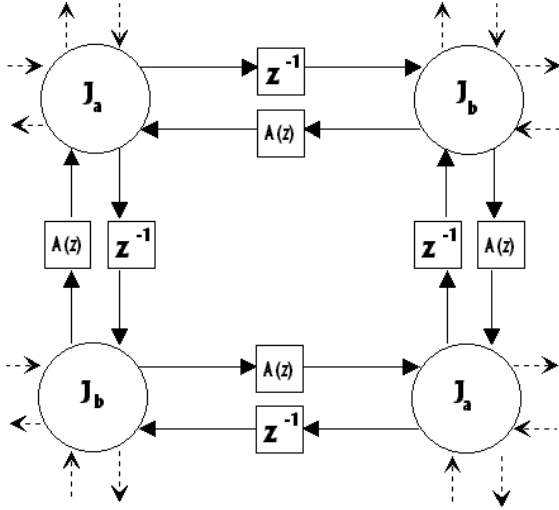


Figure 6: Unit cell in the asymmetrically warped waveguide mesh.

5.3. The Mass-Loaded Mesh

The next approach we consider is warping the propagation speed on the mesh by adding a reactive load to each junction. A purely reactive load will affect dispersion but not dissipation on the mesh. It, in effect, creates a variable wave speed for different frequencies and thus warps the mesh. The simplest load that warps propagation speed in the right direction is a free mass attached to a waveguide junction, as shown in Fig. ??.

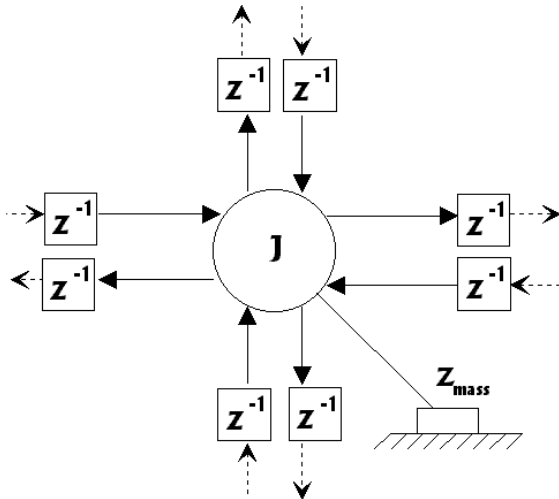


Figure 7: Mass loaded mesh.

The motivation behind this is that adding such a mass to each junction “stiffens” the mesh, and stiffness introduces dispersion in a 2D membrane which speeds up high-frequency propagation, as needed. The mass is chosen so that the dispersion introduced by stiffness cancels as much as possible the dispersion due to quantization of direction in the 2D membrane. Adding a load to a junction can be done by adding an impedance to the junction. This modifies the normal junction velocity to

$$V_J = \frac{2 * R}{\sum_i R_i + R_J} \sum_i R_i V_i^+, \quad (2)$$

where the R_i are the impedances from the delay lines coming into the junction. These all have the same value for an isotropic mesh. R_J is the junction impedance for which a mass impedance will be taken. The driving-point impedance of an ideal physical mass is given by

$$R_k(s) = m * s \quad (3)$$

where m is the weight of the mass and s is the Laplace transform variable. To adapt this impedance to a discrete-time simulation, we have to transform it to the z -domain. This can be done via the bilinear transformation:

$$s = \frac{2}{T} \frac{1 - z^{-1}}{1 + z^{-1}}$$

where T is the discrete-time sampling interval. Now the z -transform of the mass impedance is

$$R_m(z) = \frac{mT}{2} \frac{1 - z^{-1}}{1 + z^{-1}}. \quad (4)$$

Using the z -transform of the mass impedance and the formula for the loaded junction velocity, we can derive the equation for the junction velocity in the case of mass loading:

$$v_J(n) = \frac{2R}{NR + m} \sum_i [v_i^+(n) + v_i^+(n-1)] + \frac{NR - m}{NR + m} v_J(n-1)$$

where m is the weight for the load, R the impedance of the connected waveguides and N is the number of ports. Without loss of generality we can assume $R = 1$. Using this structure, we can see that for the deinterpolated mesh we need 10 extra additions and two extra multiplications per waveguide mesh junction, and for the triangular mesh we need 7 extra additions and two extra multiplies. The warping can be made more ‘interesting’ by using a first-order allpass warping on the mass impedance. The following equation uses this allpass warping in the deinterpolated mesh:

$$v_J(n) = \alpha \sum_i h_i [v_i^+(n) + v_i^+(n-1)] + \beta v_J(n-1)$$

$$\alpha = \frac{2(1 - \lambda)}{H(1 - \lambda) + m(1 + \lambda)}$$

$$\beta = \frac{m(1 + \lambda) - H(1 - \lambda)}{H(1 - \lambda) + m(1 + \lambda)}$$

Adjusting the mass m or the warping parameter λ gives another expression for the junction velocity.

5.4. Wave Digital Mass Loading

Another way to implement a mass is as a wave digital filter [?, ?]. In this formulation the mass becomes an extra self-looped port. If we use flow (as opposed to force) variables in the wave digital mass, the relationship between input and output is $a[n] = z^{-1}b[n]$, where $a[n]$ is the output at time n and $b[n]$ is the input. The waveguide mesh with wave digital mass attached is shown in Fig. ??.

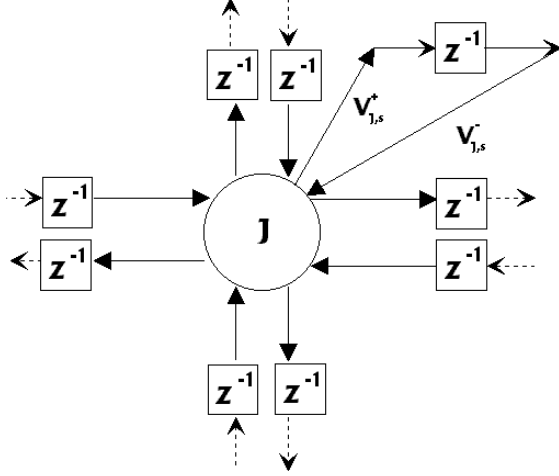


Figure 8: Mesh with wave digital mass added.

The self-loop associated with the mass load can be understood to temporarily “store” passing wave energy, thereby delaying it and slowing down wave propagation [?].

$$v_J = \frac{2}{8 + R_m} \left[\sum_{x=1}^3 \sum_{y=1}^3 h_{x,y} v_{x,y}^+ + R_m \cdot v_m^+ \right] \quad (5)$$

5.5. Equivalence between mass loading schemes

It can be shown that mass loading by adding a mass impedance to each junction and wave digital mass loading are equivalent. Starting from the expression for the loaded junction velocity with a mass load,

$$V_J(n) = \alpha (1 + z^{-1}) \sum_i h_i [V_i^+(n)] + \beta z^{-1} V_J.$$

Now $z^{-1}V_J(n)$ is added to the left- and right-hand sides to get

$$(1 + z^{-1})V_J(n) = \alpha (1 + z^{-1}) \sum_i h_i [V_i^+(n)] + (\beta + 1) z^{-1} V_J$$

Noting that $V_J = V_J^+ + V_J^-$,

$$(1 + z^{-1})V_J(n) = \alpha (1 + z^{-1}) \sum_i h_i [V_i^+(n)] + (\beta + 1) z^{-1} (V_J^+ + V_J^-)$$

Since we have a mass load, the relationship between incoming wave and reflected wave is $V_J^+ = z^{-1}V_J^-$, yielding

$$(1 + z^{-1})V_J(n) = \alpha (1 + z^{-1}) \sum_i h_i [V_i^+(n)] + (\beta + 1) z^{-1} (1 + z^{-1}) V_J^-.$$

Dividing out $(1 + z^{-1})$ gives

$$V_J(n) = \alpha \sum_i h_i [V_i^+(n)] + (\beta + 1) z^{-1} V_J^-.$$

Making the substitution $V_J^+ = (1/z^{-1})V_J^-$,

$$V_J(n) = \alpha \sum_i h_i [V_i^+(n)] + (1 + \beta) V_J^+,$$

which is the expression for a wave digital mass added to the junction. From we can derive the relation between the parameters in the two schemes. We define $\gamma = 1 + \beta = 2 \cdot \frac{k(1+\lambda)}{H(1-\lambda) + k(1+\lambda)}$

It is now shown that mass loading is the same as adding wave digital masses into the system. We can therefore treat them in a uniform way. This is not entirely unexpected, since wave digital filters also use a particular bilinear transform.

5.6. Von Neumann Analysis of the Mass Loaded Mesh

We can use Von Neumann analysis to look at the dispersion error. If we want to analyze this scheme, we first have to write down the junction transfer function:

$$V_J = \alpha \cdot z^{-1} \cdot \sum_{x=-1}^1 \sum_{y=-1}^1 h_{x,y} V_{J,x,y} + \gamma \cdot z^{-1} \cdot V_J - z^{-2} V_J \quad (6)$$

Taking the spatial Fourier transform gives

$$V(n, \varepsilon_1, \varepsilon_2) = [\alpha \cdot \sum_{x=-1}^1 \sum_{y=-1}^1 h_{x,y} \cdot e^{x \cdot \omega_1 + y \cdot \omega_2} + \gamma] \cdot V(n-1, \varepsilon_1, \varepsilon_2) - V(n-2, \varepsilon_1, \varepsilon_2)$$

The spectral amplification factor is found to satisfy

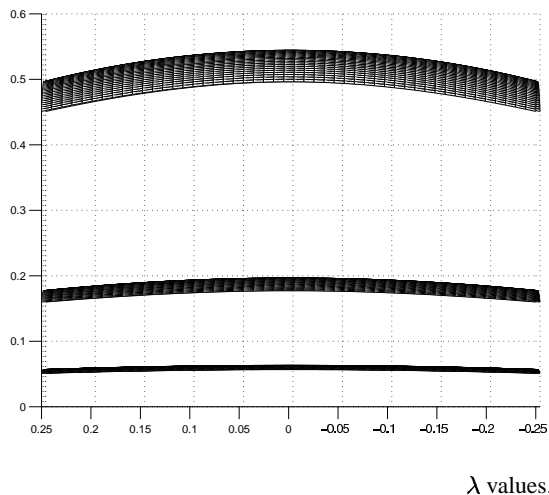
$$g(\varepsilon_1, \varepsilon_2)^2 = g(\varepsilon_1, \varepsilon_2) * b(\varepsilon_2, \varepsilon_2) - 1$$

where

$$b(\varepsilon_2, \varepsilon_2) = \alpha \cdot 2 \cdot [h_d (\cos \xi_1 cT + \cos \xi_2 cT) + h_h (\cos \omega_1 cT + \cos \omega_2 cT) + h_s + \gamma]$$

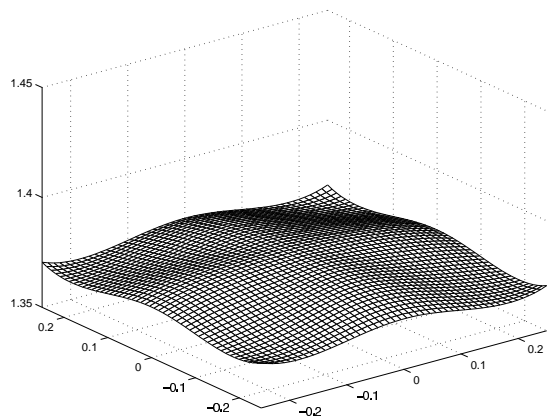
In this formula h_h are the multiplication factors along the horizontal direction h_d along the diagonal directions and h_s the multiplication factor from the self loop. The dispersion on the mass-warped mesh is therefore

$$k(\varepsilon_1, \varepsilon_2) = \frac{c'(\varepsilon_1, \varepsilon_2)}{c} = \frac{\sqrt{2}}{2\pi\varepsilon} \arctan \frac{\sqrt{4 - b(\varepsilon_1, \varepsilon_2)^2}}{b(\varepsilon_1, \varepsilon_2)} \quad (8)$$



In this simulation, the value for m was taken to be 1 while λ was varied. The values for λ in this simulation were 0.9, 0.99 and 0.999. The mesh that has the most dispersion at DC is $\lambda = 0.9$ and then going progressively down to 0.999. For λ going to 1 the dispersion error becomes completely flat.

In section ?? it was seen that adding a self loop to a junction slows down or speeds up the wave propagation. In the deinterpolated mesh a wave digital mass is used. This can be used in parallel with the wave digital mass we just developed to speed up the waves a little. This speeding up is done by varying $h_{0,0} = h_s$ which is the multiplication factor in the deinterpolated mesh. We have to make sure, however, that the condition $\sum_{i,j} h_{i,j} = H$ is maintained [?].



$m = 4, h_h = 1.24814, h_d = 0.375930, h_s = -7$ and $\lambda = 0.08$. The dispersion has now become almost completely flat within the region where the spatial frequency is smaller than a quarter of the sampling frequency. (The z -axis now has a much smaller scale than in the other pictures).

5.7. Future work

To further compensate for mesh dispersion error, a variable delay (allpass filter) may be introduced into the self-loop in cascade with the unit delay (at least one sample of pure delay is needed for self-loop realizability). The allpass filter coefficients may be optimized to minimize dispersion error over a selected frequency range. Use of such an allpass filter corresponds to using higher order reactive loads on the mesh junctions.

Further optimization of all the parameters in the mass warped mesh is required to obtain optimal results.

It would be of interest to see what can be accomplished using springs instead of masses to warp the mesh.

5.8. Acknowledgment

The author would like to thank Prof. Julius Smith of CCRMA for supervising this research, for helping with the preparation of this paper, and for originally suggesting some of the basic research ideas, such as spring- or mass-loading an isotropic mesh so as to cause a partially compensating dispersion profile versus frequency.

6. REFERENCES

- [1] S. Van Duyne and J.O. Smith, "Physical modeling with the 2-D digital waveguide mesh," in Proc. Int. Comp. Music Conference (ICMC'93), Tokyo, Japan, Sept. 1993, pp. 40-47
- [2] L. Savioja and V. Välimäki, "The bilinearly deinterpolated waveguide mesh", Proc. IEEE Nordic Signal Processing symp. (NORSIG'96) Espoo, Finland, Sept. 1996, pp. 443-446
- [3] L. Savioja and V. Välimäki, "Reduction of the dispersion error in the interpolated digital waveguide mesh using frequency warping", Proc. Int. Conf. Acoust., Speech and Signal Processing (ICASSP'99), vol. 2, Phoenix, AZ, Mar. 15-19, 1999, pp. 973-976.
- [4] L. Savioja and V. Välimäki, "Reducing the Dispersion Error in the Digital Waveguide Mesh Using Interpolation and Frequency-Warping Techniques", IEEE Trans. Speech and Audio Proc., pp. 184-194, March, 2000.
- [5] F. Fontana and D. Rocchesso, "Physical modeling of membranes for percussion instruments", Acustica, vol. 84, no. 3, pp. 529-542, May/June 1998.
- [6] L. Savioja and J. Backman and A. Järvinen and T. Takala, "Waveguide mesh method for low-frequency simulation of room acoustics", in Proc. 15th Int. Congress on Acoustics (ICA-95), Trondheim, Norway, pp. 637-640, June, 1995.
- [7] S. Bilbao, "Wave and Scattering Methods for the Numerical Integration of Partial Differential Equations", Ph.D. thesis, Electrical Engineering Department (CCRMA), Stanford University, Stanford, CA 94305, forthcoming.
- [8] A. Fettweis, "Wave Digital Filters: Theory and Practice", Proc. IEEE, vol. 74, no. 2, pp. 270-327, Feb. 1986.
- [9] J. Strikwerda, "Finite difference schemes and partial differential equations", Wadsworth & Brooks, Pacific Grove, CA